Journal of Dental Research
2015, Vol. 94(5) 715–721

DOI: 10.1177/0022034515570943
jdr.sagepub.com

Functional Differences in the Acinar Cells of the Murine Major Salivary Glands

Y. Kondo[1,2], T. Nakamoto[2], Y. Jaramillo[1], S. Choi[1], M.A. Catalan[1], and J.E. Melvin[1]

Abstract

In humans, approximately 90% of saliva is secreted by the 3 major salivary glands: the parotid (PG), the submandibular (SMG), and the sublingual glands (SLG). Even though it is known that all 3 major salivary glands secrete saliva by a Cl^--dependent mechanism, salivary secretion rates differ greatly among these glands. The goal of this study was to gain insight into the properties of the ion-transporting pathways in acinar cells that might account for the differences among the major salivary glands. Pilocarpine-induced saliva was simultaneously collected in vivo from the 3 major salivary glands of mice. When normalized by gland weight, the amount of saliva secreted by the PG was more than 2-fold larger than that obtained from the SMG and SLG. At the cellular level, carbachol induced an increase in the intracellular [Ca^{2+}] that was more than 2-fold larger in PG and SMG than in SLG acinar cells. Carbachol-stimulated Cl^- efflux and the protein levels of the Ca^{2+}-activated Cl^- channel TMEM16A, the major apical Cl^- efflux pathway in salivary acinar cells, were significantly greater in PG compared with SMG and SLG. In addition, we evaluated the transporter activity of the Na^+-K^+-2Cl^- cotransporters (NKCC1) and anion exchangers (AE), the 2 primary basolateral Cl^- uptake mechanisms in acinar cells. The SMG NKCC1 activity was about twice that of the PG and more than 12-fold greater than that of the SLG. AE activity was similar in PG and SLG, and both PG and SLG AE activity was about 2-fold larger than that of SMG. In summary, the salivation kinetics of the 3 major glands are distinct, and these differences can be explained by the unique functional properties of each gland related to Cl^- movement, including the transporter activities of the Cl^- uptake and efflux pathways, and intracellular Ca^{2+} mobilization.

Keywords: epithelia, physiology, salivary physiology, chloride channel, Na-K-Cl transporter, calcium signaling

Introduction

Saliva secreted by exocrine salivary glands protects the health of the hard and soft tissues of the oral cavity and upper gastrointestinal tract. Mammals have 3 pairs of major salivary glands, the parotid, submandibular, and sublingual glands, along with numerous minor salivary glands located throughout the oral, lingual, and labial mucosae. Salivary glands appear histologically similar, being composed mainly of acinar and duct cells. Acinar cells can be either serous or mucus, whereas the ducts are largely composed of intercalated and striated cells.

Human salivary glands secrete from 0.5 to 1 liter of saliva per day. In brief, acinar cells initially produce an isotonic, plasma-like fluid that is further modified by duct cells by reabsorbing most of the NaCl and secreting $KHCO_3$. Because the ducts are relatively impermeable to water, the final saliva is hypotonic. Fluid secretion is mainly triggered by an increase in the intracellular Ca^{2+} concentration, which activates apical Ca^{2+}-activated Cl^- channels that promote luminal Cl^- accumulation, the driving force for Na^+ and water movement through the tight junction complex and apical water channels, respectively (Nauntofte 1992; Melvin et al. 2005).

Although all 3 major salivary glands appear to secrete fluid by a similar molecular mechanism, the amount and composition of their secretion products differ greatly. It has been estimated that during unstimulated periods 20% of human whole saliva originates from the parotid gland, 65% from the submandibular, 7 to 8% from the sublingual, and the remainder from minor glands (Edgar 1990). In contrast, the contributions of the parotid glands dramatically increase during stimulation (Dawes and Wood 1973; Edgar 1990; Proctor and Carpenter 2007). In the present study, we compared the amounts of fluid and the activities of the ion-transporting proteins involved in saliva secretion in the major mouse salivary glands. Our results demonstrate that the amount of fluid secreted normalized by gland weight significantly differs among the major salivary glands. These differences appear to be related to differences in the magnitude of Ca^{2+} signaling evoked in response to

[1]Secretory Mechanisms and Dysfunction Section, National Institute of Dental and Craniofacial Research, National Institutes of Health, Bethesda, MD, USA
[2]Department of Oral Reconstruction and Rehabilitation, Kyushu Dental University, Kitakyushu, Fukuoka, Japan

A supplemental appendix to this article is published electronically only at http://jdr.sagepub.com/supplemental.

Corresponding Author:
J.E. Melvin, Secretory Mechanisms and Dysfunction Section, National Institute of Dental and Craniofacial Research, National Institutes of Health, 10 Center Drive, Building 10/Room 1N117B, Bethesda, MD 20892, USA.
Email: james.melvin@nih.gov

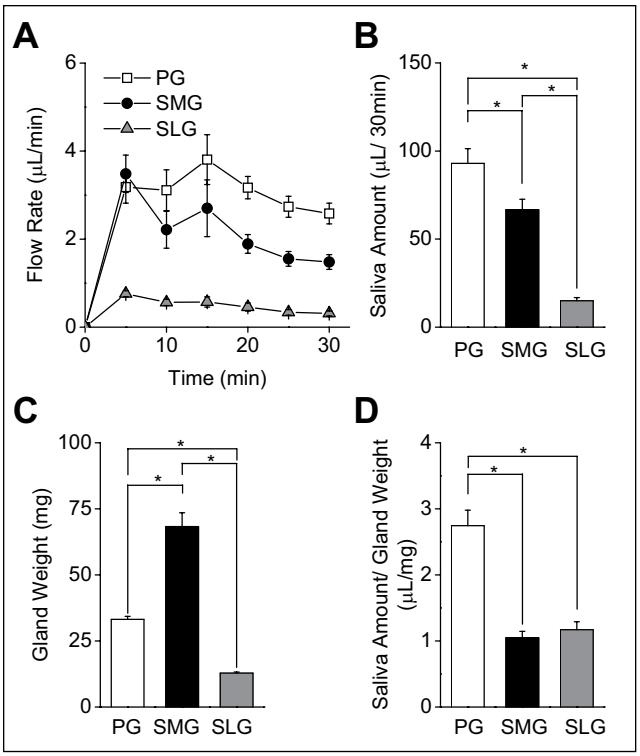

Figure 1. Pilocarpine induced in vivo salivation from mouse parotid (PG), submandibular (SMG), and sublingual glands (SLG). (**A**) Flow rate (µL/min) of pilocarpine (10 mg/kg)-stimulated, gland-specific saliva was collected for 30 min from PG (open squares), SMG (filled circles), and SLG (gray triangles). (**B**) Total amount of secreted saliva during 30 min of stimulation (µL/30 min). Secreted saliva was significantly greater in PG, followed by SMG and SLG. (**C**) Average gland weight (mg) was significantly greater in SMG, followed by PG and SLG. (**D**) Amount of saliva normalized by gland weight (µL/mg). Saliva amount per gland weight was significantly greater in PG than in SMG and SLG, while SMG and SLG were not different. One-way ANOVA followed by Bonferroni's post hoc test was applied for the detection of statistically significant differences. *$P < 0.05$; $n = 24$ (males = 12, females = 12).

stimulation as well as to the distinct activities of Cl^- transporters linked to saliva secretion.

Materials and Methods

Mice were housed in cages with access to laboratory chow and water ad libitum with a 12-hour light/dark cycle. Gene targeting and genotyping protocols were performed as described for *Nkcc1* (Flagella et al. 1999), ACID (Flodby et al. 2010), and $ROSA^{mT/mG}$ mice (Muzumdar et al. 2007) (The Jackson Laboratory, Bar Harbor, ME, USA). Equal numbers of sex- and age-matched (from 6 to 24 wk old) mice were utilized. All animal procedures were approved by the Animal Care and Use Committee of the National Institute of Dental and Craniofacial Research, National Institutes of Health (ASP 13-686). The ion-sensitive fluorescent indicators SNARF1-AM, Fluo4-AM, SPQ, and Fura red-AM were from Invitrogen (Carlsbad, CA, USA). Liberase TL was from Roche Life Science (Indianapolis, IN, USA). All other reagents were from Sigma-Aldrich (St. Louis, MO, USA), unless otherwise indicated. Procedures for obtaining salivary gland tissue slices, dispersed cells, Western blotting, and imaging experiments are fully described in the Appendix Materials and Methods section.

Statistical Analysis

Results are presented as the mean ± SEM. Statistical significance was determined by one-way analysis of variance (ANOVA) followed by Bonferroni's post hoc test. *P* values of less than 0.05 were considered statistically significant. Origin 7.0 Software was used for statistical calculations (OriginLab, Northampton, MA, USA). All experiments were performed with preparations from 4 or more different mice for each condition.

Results

In Vivo Pilocarpine-induced Salivation from the 3 Major Mouse Salivary Glands

Together, the parotid (PG), submandibular (SMG), and sublingual (SLG) glands produce about 90% of the oral fluid, but the relative contribution that each exocrine gland makes to this process has not been directly compared. For simultaneous comparison of the in vivo secretion flow rates of each gland type, pilocarpine-stimulated saliva was collected from the 3 major salivary glands in individual mice. Figure 1A shows that the in vivo secretion rates in response to the cholinergic receptor agonist pilocarpine (10 mg/kg body weight) were relatively constant for all 3 glands over the 30-minute stimulation period. As summarized in Figure 1B, the total amount of saliva secreted during the 30-minute period by the PG was approximately 30% higher than that by the SMG and 6-fold higher than that by the SLG.

If the secretory machinery is functionally equivalent in the 3 major salivary glands, it might be expected that the amount of saliva generated would directly correlate with gland weight. Figure 1C shows that the weight of the SMG is more than twice that of the PG and nearly 7-fold larger than that of the SLG (PG: SMG: SLG = 1: 2.12: 0.31, respectively, normalized to PG weight). Consequently, when the total saliva generated by each gland was normalized to its gland weight, the PG was greater than 2-fold more efficient in secreting fluid than were the SMG and SLG, while the SMG and SLG were not significantly different (Fig. 1D).

Acinar and Ductal Composition of Mouse Salivary Glands

Figure 1D demonstrates that, when normalized to gland weight, the mouse PG secretes significantly more fluid in response to stimulation than does either the SMG or SLG. One possible explanation for this apparent functional difference is that the glandular volume of secretory acinar cells relative to duct cells is considerably greater in the PG. Salivary glands are composed primarily of 2 general cell types, the fluid-secreting acinar cells and

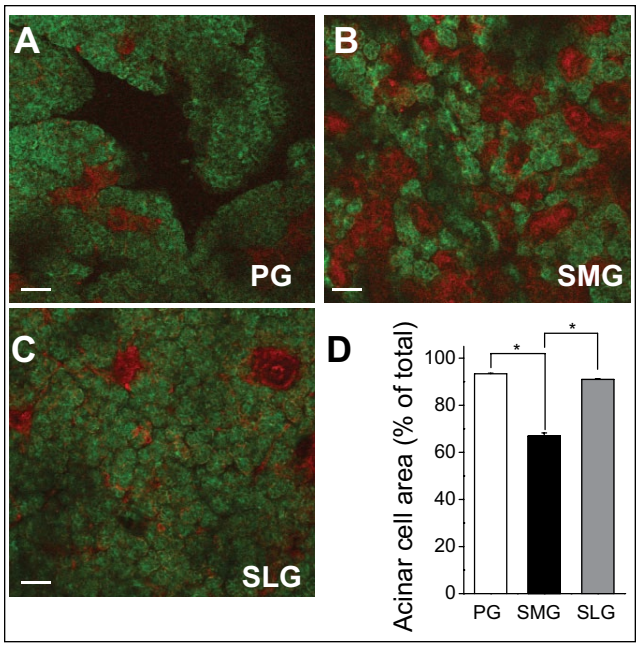

Figure 2. Acinar and ductal cross-sectional areas in mouse parotid (PG), submandibular (SMG), and sublingual glands (SLG). Salivary gland tissue slices from ACID/ROSA$^{mT/mG}$ mice were used to estimate the acinar and ductal cross-sectional areas in mouse PG, SMG, and SLG. ACID/ROSA$^{mT/mG}$ mice express green fluorescent acinar regions and red fluorescent ducts. (**A–C**) Fluorescence images of mouse PG, SMG, and SLG, respectively. (**D**) Summary of acinar and ductal areas in PG, SMG, and SLG. Acinar cross-sectional areas in PG and SLG were significantly larger than in SMG. One-way ANOVA followed by Bonferroni's post hoc test was applied for the detection of statistically significant differences. *$P < 0.05$; $n = 6$ (males = 3, females = 3). Bars = 50 µm.

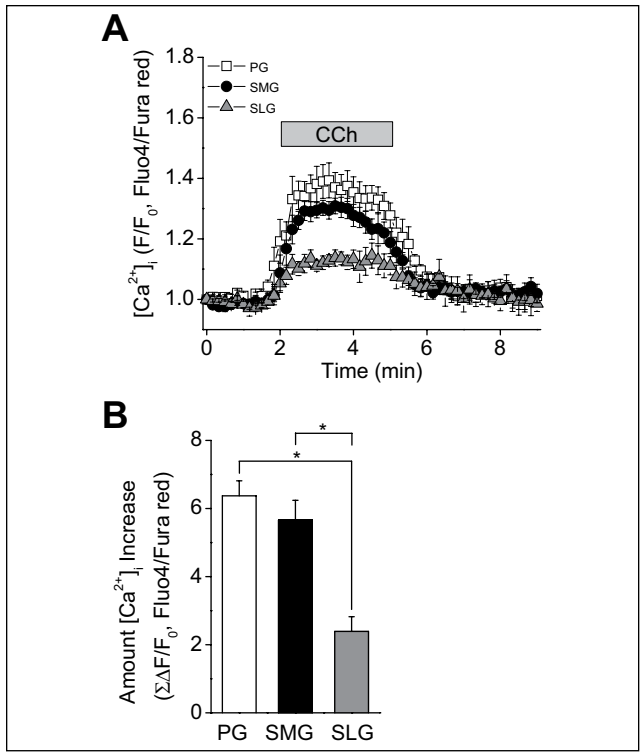

Figure 3. Muscarinic stimulation induced $[Ca^{2+}]_i$ increase in mouse parotid (PG), submandibular (SMG), and sublingual (SLG) acinar cells. $[Ca^{2+}]_i$ was measured in Fluo4- and Fura Red-loaded tissue slices. (**A**) Time-course of the $[Ca^{2+}]_i$ increase in response to 0.3 µM Carbachol (CCh, when indicated by the bar) in mouse (C57BL6) PG, SMG, and SLG acinar cells. (**B**) Magnitude of the $[Ca^{2+}]_i$ increase during stimulation in mouse acinar cells calculated from the area under the curve. PG and SMG showed significantly greater stimulated $[Ca^{2+}]_i$ increases than did SLG. One-way ANOVA followed by Bonferroni's post hoc test was applied for the detection of statistically significant differences. *$P < 0.05$. $n = 6$ (males = 3, females = 3).

the NaCl-absorbing duct cells, which secrete little if any fluid. Figures 2A, 2B, and 2C (PG, SMG, and SLG, respectively) show representative tissue sections from mice that have been genetically engineered to express fluorescent tomato red protein in duct cells, while the acinar cells specifically express green fluorescent protein (see Appendix Materials and Methods). The glandular volume of the acinar and duct cell compartments was estimated for each gland type in tissue sections from these mice. The cross-sectional areas of acinar and ductal regions were comparable for the PG and SLG (Fig. 2D, about 90% acinar and 10% ductal). In contrast, the SMG contained dramatically more duct cells (66.91% acinar and 33.09% ductal). When the total saliva generated by each gland was normalized to its % acinar volume (true acinar volume = gland weight x % acini), the PG secreted about twice the amount of saliva as the SMG and 2.4-fold greater than the SLG (1: 0.52: 0.43, respectively, normalized to PG).

Muscarinic Receptor-induced Intracellular [Ca^{2+}] Increases in Mouse Salivary Gland Acinar Cells

The above results show that the different amounts of saliva secreted by the 3 major salivary glands cannot be entirely explained by differences in gland weight or the acinar volume of the glands. Salivary gland fluid secretion depends on an increase in the intracellular free Ca^{2+} concentration ($[Ca^{2+}]_i$) (Nauntofte 1992; Ambudkar 2014) to activate many Ca^{2+}-regulated ion and water transport pathways, e.g., Ca^{2+}-activated Cl^- (Yang et al. 2008; Romanenko et al. 2010) and K^+ (Nakamoto et al. 2008) channels. Thus, we postulated that differences in Ca^{2+} signaling might contribute to the different amounts of saliva secreted by the 3 major salivary glands.

To test this hypothesis, we measured the magnitude of the $[Ca^{2+}]_i$ increase stimulated by 0.3 µM Carbachol (CCh) in Fluo4- and Fura red-loaded acinar cells in organotypic tissue slices from the 3 major salivary glands. CCh stimulation caused an increase in the $[Ca^{2+}]_i$ with similar time kinetics in the 3 glands (Fig. 3A). Likewise, the magnitude of the $[Ca^{2+}]_i$ increase, expressed as the area under the curve, was equivalent in PG and SMG (Fig. 3B); however, the $[Ca^{2+}]_i$ increase was significantly less in the SLG (~50% lower), consistent with the lower flow rates in the SLG compared with those in the PG and SMG.

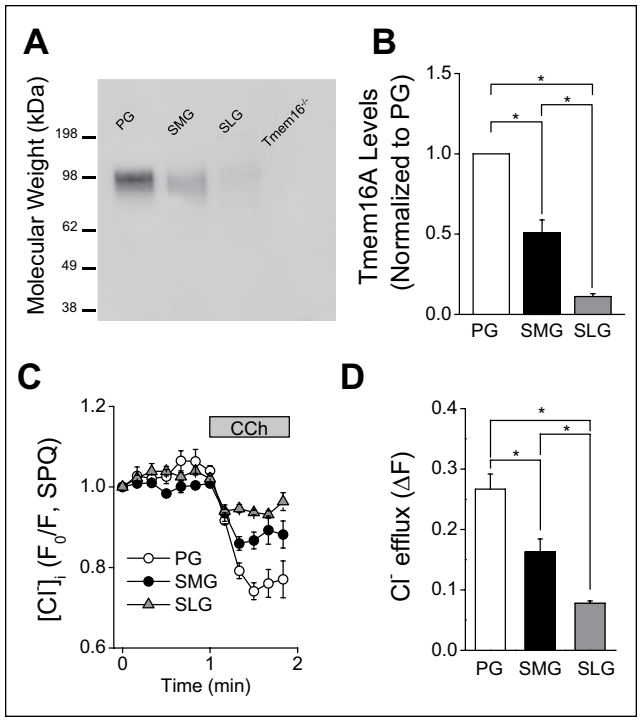

Figure 4. TMEM16A protein expression and muscarinic receptor-activated decrease in $[Cl^-]_i$ in mouse parotid (PG), submandibular (SMG), and sublingual gland (SLG) acinar cells. (**A**) Western blot analysis with an anti-TMEM16A antibody was performed as described in the "Appendix Materials and Methods" section by loading 10 µg of acinar protein/lane isolated from mouse (C57BL/6) PG, SMG, and SLG. The specificity of the anti-TMEM16A antibody was confirmed by the absence of a reactive band in the lane loaded with SMG protein from a mouse lacking TMEM16A (*Tmem16A*$^{-/-}$). (**B**) Summary of 4 independent experiments performed on individual protein samples obtained from 4 mice (2 females and 2 males). Band intensities (obtained by densitometric analysis with ImageJ software) were normalized by the intensity obtained from PG in each separate blot, which displayed the highest expression level among major salivary glands. (**C**) Changes in $[Cl^-]_i$ in response to 0.3 µM CCh were measured in SPQ-loaded cells from mouse (C57BL/6) PG, SMG, and SLG. (**D**) Summary of the magnitude of the $[Cl^-]_i$ decrease in PG, SMG, and SLG acinar cells from mouse (C57BL/6). The $[Cl^-]_i$ decrease was significantly greater in the PG, followed by the SMG and then the SLG. One-way ANOVA followed by Bonferroni's post hoc test was applied for the detection of statistically significant differences. *$P < 0.05$. $n = 4$ (males = 2, females = 2).

Functional Expression and Protein Levels of TMEM16A Cl^- Channels in Mouse Salivary Glands

Fluid secretion is driven by transepithelial Cl^- transport via basolateral Cl^- uptake and apical Cl^- efflux pathways. Two basolateral Cl^- uptake pathways have been implicated in this process in salivary glands, the Na^+-K^+-$2Cl^-$ cotransporter and Cl^-/HCO_3^- exchanger mechanisms (Novak and Young 1986; Melvin and Turner 1992; Nauntofte 1992; Evans et al. 2000), while the apical Cl^- efflux pathway depends on TMEM16A Ca^{2+}-activated Cl^- channel in salivary gland acinar cells (Romanenko et al. 2010). However, a direct comparison of the relative cotransporter, exchanger, and channel activities has not been done in the acinar cells of the 3 major mouse salivary glands.

First, we compared the TMEM16A expression levels among the 3 major salivary glands by Western blotting analysis (Fig. 4A) by loading the gel with equal amounts of acinar cell protein (see Appendix Materials and Methods). Figure 4B summarizes the results of the experiments like those shown in Figure 4A, and demonstrates that the level of TMEM16A protein in PG acinar cells was ~2-fold greater than that in the SMG and more than 9-fold larger than that in the SLG. In accordance with the protein expression levels, the magnitude of the 0.3 µM CCh-induced Cl^- efflux in SPQ-loaded PG acinar cells was more than 1.5-fold greater than that in the SMG and more than 3-fold larger than that in the SLG (1: 0.61: 0.29, normalized to Cl^- efflux in PG). Consequently, the TMEM16A expression levels and the magnitude of the muscarinic agonist-induced Cl^- efflux were consistent with the volume of saliva secretion from the 3 major salivary glands when normalized by acinar cell volume.

Na^+-K^+-$2Cl^-$ Cotransporter Activity in the Acinar Cells of Mouse Salivary Glands

Na^+-K^+-$2Cl^-$ cotransporter activity was examined in the acinar cells of PG, SMG, and SLG tissue slices loaded with the pH-sensitive dye SNARF1. Initial studies evaluated the level of Na^+-K^+-$2Cl^-$ cotransporter activity in the PG by determining its sensitivity to bumetanide, a Na^+-K^+-$2Cl^-$ cotransport inhibitor, and by comparing its activity in wild-type mice and mice lacking NKCC1 (*Nkcc1*$^{-/-}$ mice; Appendix Fig. 1). Exposure to 30 mM NH_4Cl (see Materials and Methods) induced a rapid intracellular alkalization. This transient intracellular alkalization was followed by a relatively slow acidification that is induced by NH_4^+ entry via K^+ pathways (NH_4^+ acts as a K^+ surrogate), including the NKCC1 Na^+-K^+-$2Cl^-$ cotransporter. The acidification observed in PG acinar cells from wild-type control mice (*Nkcc1*$^{+/+}$) was significantly inhibited by bumetanide, a selective inhibitor of Na^+-K^+-$2Cl^-$ cotransporter activity (Appendix Fig. 1A). In contrast, the acidification rate in acinar cells from *Nkcc1*$^{-/-}$ mice was insensitive to bumetanide and was comparable with the acidification rate in acinar cells from littermate *Nkcc1*$^{+/+}$ mice in the presence of bumetanide (Appendix Fig. 1B; see summary of data in Appendix Fig. 1C). Consequently, the bumetanide-sensitive component of the acidification was used to evaluate NKCC1 Na^+-K^+-$2Cl^-$ cotransporter activity in the major salivary glands.

We found significant differences in the bumetanide-sensitive acidification rates among PG, SMG, and SLG acinar cells (Fig. 5A). Note that the rates of the bumetanide-insensitive acidification were not statistically different for the 3 glands (Fig. 5A, black bars). The SMG bumetanide-sensitive Na^+-K^+-$2Cl^-$ cotransporter activity (Fig. 5B) was about twice that of the PG and more than 12-fold greater than that of the SLG (PG: SMG: SLG = 0.5: 1: 0.08, respectively, normalized to SMG cotransporter activity). Indeed, the acidification rates in the presence and absence of bumetanide were not statistically different in SLG acinar cells, suggesting that there is little functional Na^+-K^+-$2Cl^-$ cotransporter activity in mouse sublingual salivary glands.

Cl^-/HCO_3^- Exchanger Activity in Acinar Cells of Mouse Salivary Glands

We hypothesized that another Cl^- uptake mechanism might compensate for the very low Na^+-K^+-$2Cl^-$ cotransporter activity in SLG acinar cells (Fig. 5B). The other major Cl^- uptake mechanism observed in salivary acinar cells is basolateral Cl^-/HCO_3^- exchange (Turner and George 1988; Nauntofte 1992; Nguyen et al. 2004). Cl^-/HCO_3^- activity was examined in PG, SMG, and SLG slices loaded with the pH-sensitive dye SNARF1. Reduction of external Cl^- induces an intracellular alkalization in the presence of HCO_3^- as intracellular Cl^- exchanges for extracellular HCO_3^- via Cl^-/HCO_3^- exchange. The rate of this alkalization represents the Cl^-/HCO_3^- activity. Extracellular Cl^- reduction induced an alkalization (Fig. 5C), and the alkalization in all 3 glands was entirely inhibited by external HCO_3^- removal (Appendix Fig. 2), consistent with Cl^-/HCO_3^- exchanger activity in all 3 glands. The initial rate of the Cl^-/HCO_3^- exchanger activity was approximately 19% greater in SLG compared with that in PG, while SMG Cl^-/HCO_3^- exchanger activity was about 50% of that observed in the PG and SLG (Fig. 5D, PG: SMG: SLG = 1.0: 0.54: 1.19, respectively, normalized to PG exchanger activity).

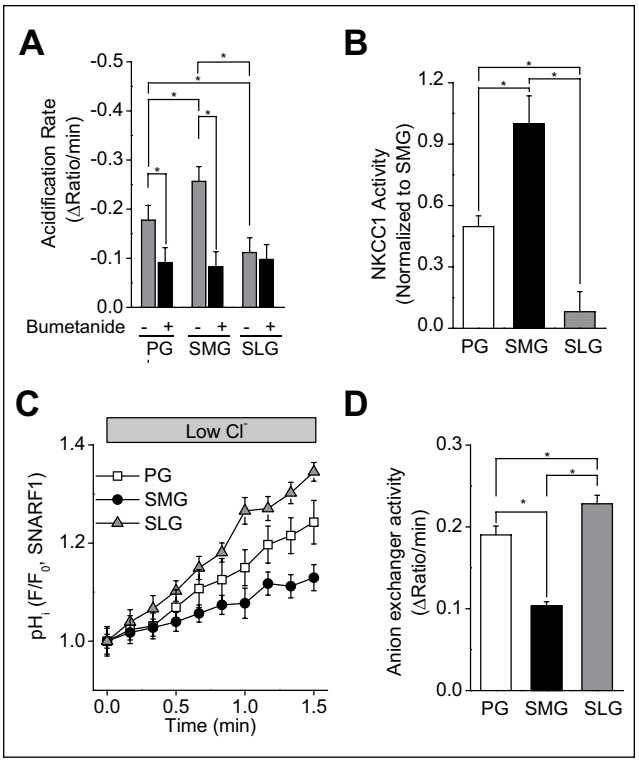

Figure 5. Na^+-K^+-$2Cl^-$ cotransporter (NKCC1) and Cl^-/HCO_3^- anion exchanger activities in mouse parotid (PG), submandibular (SMG), and sublingual gland (SLG) acinar cells. Intracellular pH (pH_i) was measured in SNARF1-loaded tissue slices. Na^+-K^+-$2Cl^-$ cotransporter activity was monitored as the bumetanide-sensitive (50 μM of the Na^+-K^+-$2Cl^-$ cotransporter inhibitor) acidification rate following the perfusion of a 30 mM NH_4Cl containing external solution. (**A**) Summary of the acidification rates in mouse (C57BL/6) PG, SMG, and SLG acinar cells with or without bumetanide. Bumetanide decreased the acidification rate in acinar cells from SMG and PG, but had no significant effect on SLG acidification. (**B**) Summary of the bumetanide-sensitive NKCC1 activity in PG, SMG, and SLG acinar cells. NKCC1 activity was significantly greater in SMG, followed by PG and then SLG. The values were normalized to the value obtained from SMG, which displayed the highest NKCC1 activity among major salivary glands. (**C**) Representative experiments showing pH_i changes mediated by Cl^-/HCO_3^- anion exchanger activity in response to a low Cl^- solution in mouse (C57BL/6) PG (open squares), SMG (filled circles), and SLG (gray triangles) acinar cells. (**D**) Summary of the Cl^-/HCO_3^- exchanger-dependent alkalization rates in mouse (C57BL/6) PG, SMG, and SLG acinar cells. The alkalization rate was significantly greater in SLG, followed by PG and then SMG. One-way ANOVA followed by Bonferroni's post hoc test was applied for the detection of statistically significant differences.*$P < 0.05$. $n = 6$ (males = 3, females = 3).

Discussion

Oral fluid, also known as whole saliva, is primarily secreted by 3 pairs of major salivary glands in mammals, with a negligible contribution from minor salivary glands, nasal secretions, and gingival and mucosal exudates. Salivary glands are unique among exocrine glands because all glands secrete into the same compartment, where their fluids mix to define the characteristic functional properties of whole saliva. The salivary gland fluid secretion mechanism has been extensively studied in rodents (Martinez 1987; Nauntofte 1992; Melvin et al. 2005) and, to a lesser degree, in humans (Nakamoto et al. 2007). These studies treated the 3 major salivary glands as a single organ, with little or no consideration for the different secretory properties of the individual glands. Furthermore, enzymatically dispersed cells have generally been used to study salivary gland function, but salivary cells prepared under such conditions lose critical morphological and functional properties (Warner et al. 2008). Therefore, the objective of the present study was to directly compare the secretion processes in the mouse parotid, submandibular, and sublingual glands using relatively non-invasive methods, e.g., simultaneous in vivo collection of saliva from the major glands, and the measurement of ion fluxes by multi-photon microscopy in organotypic tissue slices, which maintain the original interactions and functions of salivary gland acinar cells. The only exception is that we used enzymatically dispersed acinar cells to measure $[Cl^-]_i$, because slice preparations failed to load sufficiently with the poorly cell-permeable Cl^--sensitive dye SPQ.

The in vivo time kinetics of muscarinic-induced saliva secretion was similar in the 3 major mouse salivary glands during 30 min of stimulation, but the total amounts of secreted saliva were significantly different (Fig. 1B). The PG secreted approximately 30% more saliva than did the SMG and > 6-fold more than did the SLG. The simplest explanation for these observations is that the amount of saliva generated by a specific gland correlates directly with its weight. However, when the total saliva volume was normalized to gland weight, the PG secreted 2-fold more saliva than the SMG and SLG, while the SMG and SLG were not significantly different, suggesting that the PG has a more robust secretory mechanism.

Salivary glands are composed primarily of 2 general cell types, the fluid-secreting acinar cells and the NaCl-absorbing

duct cells, which secrete little if any fluid. Thus, one possible explanation for this apparent functional difference is that the glandular secretory compartment volume relative to the volume of duct cells is different in the 3 major salivary glands. Indeed, correcting the gland weight for the % of acinar cells/gland revealed that the SMG and SLG secreted essentially the same amounts of saliva, suggesting that the secretory function per acinar cell is equivalent in these 2 glands. Conversely, PG secreted > 2-fold more saliva than did the SMG and SLG when normalized by acinar cell volume.

So why do PG acinar cells secrete significantly more saliva than do the SMG and SLG? Salivary gland fluid secretion is a complex process that depends on an increase in the intracellular free Ca^{2+} concentration ($[Ca^{2+}]_i$) to initiate secretion (Nauntofte 1992; Ambudkar 2014). The increase in $[Ca^{2+}]_i$ activates Ca^{2+}-regulated ion and water transport pathways, e.g., Ca^{2+}-activated Cl^- (Caputo et al. 2008; Schroeder et al. 2008; Yang et al. 2008; Romanenko et al. 2010) and K^+ (Nakamoto et al. 2008) channels. Thus, we postulated that differences in Ca^{2+} signaling might contribute to the differences in the amounts of saliva secreted by the PG compared with the SMG and SLG. Consistent with this hypothesis, the agonist-induced intracellular Ca^{2+} increase was significantly smaller in SLG acinar cells (Fig. 3B). Conversely, the agonist-induced intracellular Ca^{2+} increase was essentially the same in the PG and SMG, suggesting that Ca^{2+} mobilization is not responsible for the fluid secretion differences between these latter 2 glands.

Because $[Ca^{2+}]_i$ mobilization in the 3 glands did not appear to correlate in all cases with differences in fluid secretion, we next explored the possibility that the Cl^- uptake and efflux pathways involved in transacinar Cl^- movement, the driving force for fluid secretion, might be involved. Cl^- uptake pathways elevate the intracellular Cl^- concentration above its electrochemical equilibrium to promote Cl^- efflux when the apical conductive pathway is activated. The NKCC1 Na^+-K^+-$2Cl^-$ cotransporter, a member of the mammalian, cation-chloride cotransporter family (Haas 1989; Haas 1994), is expressed in the basolateral membrane of acinar cells. Disruption of *Nkcc1* gene expression causes severe hyposalivation in mouse parotid glands (Evans et al. 2000). In the present study, the bumetanide-sensitive NKCC1 activity was 2-fold greater in the SMG than in the PG (Fig. 5B), demonstrating that this pathway is not responsible for the greater fluid production by the PG. Surprisingly, there was almost no NKCC1 activity in the SLG. This observation suggested that another Cl^- uptake pathway(s) must compensate for the absence of NKCC1 activity in the SLG. Indeed, the other major Cl^- uptake mechanism expressed in salivary acinar cells is the basolateral Cl^-/HCO_3^- anion exchanger (Novak and Young 1986; Pirani et al. 1987; Melvin and Turner 1992; Nguyen et al. 2004). We found that the SLG has anion exchanger activity greater than that of the PG and SMG (Fig. 5D). This result is consistent with a previous report that anion exchanger activity is significantly greater in sublingual than in mouse parotid acinar cells (Nguyen et al. 2004).

TMEM16A is a Ca^{2+}-activated Cl^- channel highly expressed in SMG acinar cell apical membranes (Yang et al. 2008; Romanenko et al. 2010). Romanenko et al. reported that TMEM16A is the acinar Ca^{2+}-activated Cl^- channel essential for saliva production. Here we show that both TMEM16A protein expression and the muscarinic agonist-induced Cl^- efflux mediated by this channel were greater in PG acinar cells than in SMG and SLG (Figs. 4B, 4D). These results demonstrate that the TMEM16A Ca^{2+}-activated Cl^- channel plays an essential secretion function in salivary acinar cells. Indeed, the amount of saliva directly correlates with TMEM16A expression and activity.

Collectively, our findings demonstrate that the PG and SMG likely secrete greater volumes of fluid than do the SLG because they display a larger increase in the intracellular $[Ca^{2+}]$ in response to stimulation, and more TMEM16A Cl^- channel and NKCC1 Na^+-K^+-$2Cl^-$ cotransporter activity. In contrast, the SLG secretes less fluid, but Cl^-/HCO_3^- exchanger activity is greater in the SLG, possibly in an attempt to compensate for less NKCC1 activity. It is important to note that the acinar cells in rodent PG, SMG, and SLG are primarily serous, seromucous, and mucous cell types, respectively. Thus, the differences in ion transporter activity may reflect unique functions of 3 different cell types.

Author Contributions

Y. Kondo, M.A. Catalan, contributed to conception, design, data acquisition, analysis, and interpretation, drafted and critically revised the manuscript; T. Nakamoto, contributed to conception, design, data acquisition, analysis, and interpretation, critically revised the manuscript; Y. Jaramillo, S. Choi, contributed to conception, data acquisition, analysis, and interpretation, critically revised the manuscript; J.E. Melvin, contributed to design, data acquisition, analysis, and interpretation, drafted and critically revised the manuscript. All authors gave final approval and agree to be accountable for all aspects of the work.

Acknowledgments

The Secretory Mechanisms and Dysfunction Section is supported by the Intramural Research Program of the National Institutes of Health [NIH, National Institute of Dental and Craniofacial Research (NIDCR)]. We are thankful to Drs. Z. Borok, E.D. Crandall, and U.P. Flodby for providing the ACID mice and to Dr. Natalie Porat-Shliom for helping with the data analysis using ImageJ software. The authors declare no potential conflicts of interest with respect to the authorship and/or publication of this article.

References

Ambudkar IS. 2014. Ca(2)(+) signaling and regulation of fluid secretion in salivary gland acinar cells. Cell Calcium. 55(6):297–305.

Caputo A, Caci E, Ferrera L, Pedemonte N, Barsanti C, Sondo E, Pfeffer U, Ravazzolo R, Zegarra-Moran O, Galietta LJ. 2008. TMEM16A, a membrane protein associated with calcium-dependent chloride channel activity. Science. 322(5901):590–594.

Dawes C, Wood CM. 1973. The contribution of oral minor mucous gland secretions to the volume of whole saliva in man. Arch Oral Biol. 18(3):337–342.

Edgar WM. 1990. Saliva and dental health. Clinical implications of saliva: report of a consensus meeting. Br Dent J. 169(3-4):96–98.

Evans RL, Park K, Turner RJ, Watson GE, Nguyen HV, Dennett MR, Hand AR, Flagella M, Shull GE, Melvin JE. 2000. Severe impairment of salivation

in Na+/K+/2Cl- cotransporter (NKCC1)-deficient mice. J Biol Chem. 275(35):26720–26726.

Flagella M, Clarke LL, Miller ML, Erway LC, Giannella RA, Andringa A, Gawenis LR, Kramer J, Duffy JJ, Doetschman T, et al. 1999. Mice lacking the basolateral Na-K-2Cl cotransporter have impaired epithelial chloride secretion and are profoundly deaf. J Biol Chem. 274(38):26946–26955.

Flodby P, Borok Z, Banfalvi A, Zhou B, Gao D, Minoo P, Ann DK, Morrisey EE, Crandall ED. 2010. Directed expression of Cre in alveolar epithelial type 1 cells. Am J Respir Cell Mol Biol. 43(2):173–178.

Haas M. 1989. Properties and diversity of (Na-K-Cl) cotransporters. Annu Rev Physiol. 51:443–457.

Haas M. 1994. The Na-K-Cl cotransporters. Am J Physiol. 267(4 Pt 1):C869–C885.

Martinez JR. 1987. Ion transport and water movement. J Dent Res. 66(Spec No):638–647.

Melvin JE, Turner RJ. 1992. Cl- fluxes related to fluid secretion by the rat parotid: involvement of Cl(-)-HCO3- exchange. Am J Physiol. 262(3 Pt 1):G393–G398.

Melvin JE, Yule D, Shuttleworth T, Begenisich T. 2005. Regulation of fluid and electrolyte secretion in salivary gland acinar cells. Annu Rev Physiol. 67:445–469.

Muzumdar MD, Tasic B, Miyamichi K, Li L, Luo L. 2007. A global double-fluorescent Cre reporter mouse. Genesis. 45(9):593–605.

Nakamoto T, Srivastava A, Romanenko VG, Ovitt CE, Perez-Cornejo P, Arreola J, Begenisich T, Melvin JE. 2007. Functional and molecular characterization of the fluid secretion mechanism in human parotid acinar cells. Am J Physiol Regul Integr Comp Physiol. 292(6):R2380–R2390.

Nakamoto T, Romanenko VG, Takahashi A, Begenisich T, Melvin JE. 2008. Apical maxi-K (KCa1.1) channels mediate K+ secretion by the mouse submandibular exocrine gland. Am J Physiol Cell Physiol. 294(3):C810–C819.

Nauntofte B. 1992. Regulation of electrolyte and fluid secretion in salivary acinar cells. Am J Physiol. 263(6 Pt 1):G823–G837.

Nguyen HV, Stuart-Tilley A, Alper SL, Melvin JE. 2004. Cl(-)/HCO(3)(-) exchange is acetazolamide sensitive and activated by a muscarinic receptor-induced [Ca(2+)](i) increase in salivary acinar cells. Am J Physiol Gastrointest Liver Physiol. 286(2):G312–G320.

Novak I, Young JA. 1986. Two independent anion transport systems in rabbit mandibular salivary glands. Pflügers Arch 407(6):649–656.

Pirani D, Evans LA, Cook DI, Young JA. 1987. Intracellular pH in the rat mandibular salivary gland: the role of Na-H and Cl-HCO3 antiports in secretion. Pflügers Arch. 408(2):178–184.

Proctor GB, Carpenter GH. 2007. Regulation of salivary gland function by autonomic nerves. Auton Neurosci. 133(1):3–18.

Romanenko VG, Catalán MA, Brown DA, Putzier I, Hartzell HC, Marmorstein AD, Gonzalez-Begne M, Rock JR, Harfe BD, Melvin JE. 2010. Tmem16A encodes the Ca2+-activated Cl- channel in mouse submandibular salivary gland acinar cells. J Biol Chem. 285(17):12990–13001.

Schroeder BC, Cheng T, Jan YN, Jan LY. 2008. Expression cloning of TMEM16A as a calcium-activated chloride channel subunit. Cell. 134(6):1019–1029.

Turner RJ, George JN. 1988. Cl(-)-HCO3- exchange is present with Na+-K+-Cl- cotransport in rabbit parotid acinar basolateral membranes. Am J Physiol. 254(3Pt1):C391–C396.

Warner JD, Peters CG, Saunders R, Won JH, Betzenhauser MJ, Gunning WT 3rd, Yule DI, Giovannucci DR. 2008. Visualizing form and function in organotypic slices of the adult mouse parotid gland. Am J Physiol Gastrointest Liver Physiol. 295(3):G629–G640.

Yang YD, Cho H, Koo JY, Tak MH, Cho Y, Shim WS, Park SP, Lee J, Lee B, Kim BM, et al. 2008. TMEM16A confers receptor-activated calcium-dependent chloride conductance. Nature. 455(7217):1210–1215.